HHS Public Access

Author manuscript

Dev Dyn. Author manuscript; available in PMC 2015 March 23.

Published in final edited form as:

Dev Dyn. 2011 July ; 240(7): 1716–1726. doi:10.1002/dvdy.22665.

CELL ADHESION MOLECULE CADHERIN-6 FUNCTION IN ZEBRAFISH CRANIAL AND LATERAL LINE GANGLIA DEVELOPMENT

Q. Liu[1], **M. R. Dalman**[1], **S. Sarmah**[2], **S. Chen**[1], **Y. Chen**[1], **A. K. Hurlbut**[1], **M. A. Spencer**[1], **L. Pancoe**[1], and **J. A. Marrs**[2,*]

[1]Department of Biology, Integrated Bioscience Program, University of Akron, Akron, OH 44325

[2]Department of Biology, Center for Regenerative Biology and Medicine, Indiana University-Purdue University Indianapolis, Indianapolis, IN 46202

Abstract

Cadherins regulate the vertebrate nervous system development. We previously showed that cadherin-6 message (*cdh6*) was strongly expressed in the majority of the embryonic zebrafish cranial and lateral line ganglia during their development. Here, we present evidence that *cdh6* has specific functions during cranial and lateral line ganglia and nerve development. We analyzed the consequences of *cdh6* loss-of-function on cranial ganglion and nerve differentiation in zebrafish embryos. Embryos injected with zebrafish *cdh6* specific antisense morpholino oligonucleotides (MOs, which suppress gene expression during development; *cdh6* morphant embryos) displayed a specific phenotype, including (i) altered shape and reduced development of a subset of the cranial and lateral line ganglia (e.g. the statoacoustic ganglion and vagal ganglion) and (ii) cranial nerves were abnormally formed. This data illustrates an important role for *cdh6* in the formation of cranial ganglia and their nerves.

Keywords

differentiation; statoacoustic ganglia; peripheral nervous system; cranial and lateral line nerves

Introduction

Similar to other vertebrates, zebrafish cranial and lateral line ganglia derive from neural crest and epidermal placodes (Northcutt and Gans, 1983; Hall, 1999; Kelsh and Raible, 2002). Anatomy and development of these ganglia in zebrafish are well-documented (Metcalfe, 1985; Raible and Kruse, 2000), but molecular mechanisms underlying their formation are still largely unknown. bHLH transcription factors NeuroD and neurogenin1 (Ma et al., 1998; Kim et al., 2001; Andermann et al., 2002), the winged-helix transcription factor Foxd3 (Lopez-Schier et al., 2004), chemokine molecule Sdf-1 and its receptor Cxcr4b (Knaut et al., 2005; Haas and Gilmour, 2006) and cell adhesion molecules, including

*To whom correspondence should be addressed. Phone: 317-278-0031; Fax: 317-274-2846; jmarrs@iupui.edu.

cadherins (see below) are implicated in cranial ganglia and/or lateral line system developmental mechanisms.

Cadherins mediate cell adhesion mainly through homophilic interactions, and they play important roles in the development of a variety of tissues and organs (Takeichi, 1991; Gumbiner, 2005). More than 100 cadherin gene superfamily members are identified, and they are grouped into several major subfamilies including classic cadherins (type I and type II), protocadherins, desmogleins, desmocollins, cadherin related neuronal receptors, Fats, and seven-pass transmembrane cadherins (Nollet et al., 2000; Yagi and Takeichi, 2000). Cadherin-2 (also called N-cadherin, cdh2) and cadherin-4 (also called R-cadherin, cdh4), both classic type I cadherins, regulate development of the cranial ganglia and lateral line system in zebrafish (Kerstetter et al., 2004; Babb-Clendenon et al., 2006; Wilson et al., 2007; Lamora and Voigt, 2009). In chicken, *cdh2* regulates aggregation of placode-derived cranial sensory ganglia (Shiau and Bronner-Fraser, 2009). Cadherin-6, previously known as K-cadherin, a classic type II cadherin (Nollet et al., 2000), plays a role in renal development (Xiang et al., 1994; Cho et al., 1998; Mah et al., 2000;Paul et al., 2004; Kubota et al., 2007) and eye formation (Ruan et al., 2006; Liu et al., 2008a). Most of the cranial and lateral line ganglia express *cdh6* during critical periods of their development in *Xenopus* (David and Wedlich, 2000) and zebrafish (Liu et al., 2006a), suggesting that this adhesion molecule regulates cranial ganglion and nerve development. We tested this idea by examining the consequences of *cdh6* morpholino knockdown on cranial ganglion and nerve development. Our evidence supports the hypothesis that *cdh6* participates in the formation of some, but not all cranial ganglia and their nerves. These findings suggest that other cadherins may have redundant functions that mask *cdh6* loss-of-function consequences in those cells.

Methods and Materials

Zebrafish (*Danio rerio*) embryos were obtained by breeding adult zebrafish raised and maintained as described in the Zebrafish Book (Westerfield, 2005). All animal related procedures were approved by the University of Akron and Indiana University animal care and use committees. Embryos used for whole-mount immunocytochemistry or in situ hybridization were raised in PTU (1-phenyl-2-thiourea, 0.003%) to prevent melanization.

Zebrafish *cdh6* morpholino oligonucleotides (*cdh6*MOs) were designed by and purchased from Gene Tools (Covalis, OR). Two translation blocking antisense MOs (*cdh6*MO1: 5'-AAG AAG TAC AAT CCA AGT CCT CAT C-3' (Kubota et al., 2007), *cdh6*MO2: 5'-TCC GCT CTT AGG GTG TCT TAC AGG G-3' (Liu et al., 2008a), and a MO with five-mismatched nucleotides (5-mis *cdh6*MO1: 5'-AAC AAG TAG AAT GCA ACT CCT GAT C-3') were used in this study. The MOs, dissolved in Daneau buffer (58 mM NaCl, 0.7 mM KCl, 0.4 mM $MgSo_4$, 0.6 mM $Ca(NO_3)_2$, and 5.0 mM HEPES pH 7.6), were microinjected into one- to four-cell stage embryos at 2–4 nl (6–12 ng for *cdh6*MO1 and 5-mis *cdh6*MO1, 3.4–6.8 ng for *cdh6*MO2) per embryo. For *cdh6* mRNA rescuing experiments, capped *cdh6* mRNA was synthesized from a pCS2+*cdh6*/eGFP vector (Kubota et al., 2007) using SP6 mMessage mMachine kits (Ambion, Austin, TX). *cdh6* mRNA (150 or 300 pg/embryo) was injected alone or with *cdh6*MO2 into one- to four-cell stage embryos as described above (Table 1).

Injected embryos were placed in a 400 ml plastic beaker, half filled with a mixture of filtered fish tank water and embryonic medium 3 (1:1 volume), and allowed to develop at 28.5°C until the embryos reached desired stages. Embryos for whole mount immunocytochemistry (ICC) or in situ hybridization were anesthetized in 0.02% MS-222 and fixed in 4% paraformaldehyde overnight at 4°C. The next day, embryos were washed in 1× phosphate buffered saline (PBS, pH 7.4), dehydrated in increasing concentrations of methanol and stored in 100% methanol at −20°C until use. Detailed procedure for whole mount ICC was described previously (Liu et al., 1999). Primary antibodies used were anti-acetylated tubulin (Sigma, 1:1,000 and 1:4,000 for fluorescent and peroxidase ICC methods, respectively), anti-HuC/D (Molecular Probe, Eugene, OR, 1:1,000 and 1:3,000 for fluorescent and peroxidase ICC respectively), and zn5 (Zebrafish International Resource Center, University of Oregon, 1,500 and 1:2,000 for fluorescent and peroxidase ICC methods, respectively). FITC-labeled anti-mouse IgG or Texas Red-labeled anti mouse IgG (Jackson ImmunoResearch Laboratories, West Grove, PA, 1:100) were used as the secondary antibody for fluorescent ICC. A regular anti-mouse ABC kit (Vector Laboratories, Burlingame, CA) was used for the peroxidase method, and visualization of the reaction was achieved by using a DAB kit (Vector Laboratories).

Procedures for synthesis of digoxigenin-labeled *cdh6* and *NeuroD* cRNA probes for in situ hybridization was described previously (Liu et al., 1999; Liu et al., 2006a). Detailed procedure for whole mount in situ hybridization was reported previously (Liu et al., 1999; Westerfield, 2005). Immunocytochemical detection of the digoxigenin-labeled probe was achieved by incubating embryos in an anti-digoxigenin Fab fragment antibody (conjugated to alkaline phosphatase) solution (Roche Molecular Biochemicals, Indianapolis, IN, 1:5,000), followed by incubating the embryos in an NBT/BCIP solution (Roche).

Terminal dUTP nick-end labeling (TUNEL) was performed on whole-mount embryos at 24 hpf, 35 hpf and 50 hpf using an in situ cell death detection kit (Roche), according to the manufacturer’s instructions.

For ICC, in situ hybridization and TUNEL experiments, control embryos (uninjected or embryos injected with the 5-misMO) and *cdh6* morphants were processed at the same time, side by side. Fluorescent and bright field images were obtained using a SPOT digital camera mounted on an Olympus BX51 microscope. Sizes of structures were measured in area (square microns) using the SPOT software. Laser scanning confocal microscopy was performed using a Zeiss LSM 700 (Peabody, MA) using a 20× objective, and z-stacks of x-y images were collected through the region of interest. Image volumes were processed and statoacoustic ganglion volume measurements were performed using Volocity Software (Perkin Elmer, Inc., Walther MA). Statistical analysis was performed using two-tail unpaired Student t-test.

Results

cdh6 mRNA is expressed in most of the cranial and lateral line ganglia of developing zebrafish

We previously showed that *cdh6* mRNA (*cdh6*) was expressed in most of the cranial and lateral line ganglia of embryonic zebrafish (Liu et al., 2006a). As early as 16–17 hpf, *cdh6* was expressed in the anterior lateral line placode area (a, the precursor of the anterodorsal and anteroventral lateral line ganglia, Andermann et al., 2002), and the postotic placode (PP, Fig. 1A). At about 20 hpf, cells in the anterior portion of the PP become the posterior lateral line ganglion (gP), while cells in the posterior portion of the PP begin to separate from the gP, and migrate caudally to become the primordium of the posterior lateral line (pPLL, MetCalfe, 1985; Kimmel et al., 1995). At 20–21 hpf, both the anterior lateral line placode area and the gP contained high levels of *cdh6* (Fig. 1B and C), but only a few cells in the newly formed pPLL expressed *cdh6* (Fig. 1C). At 24 hpf, *cdh6* was expressed in a subset of cells (mainly in cells in the peripheral region, not in the anterior and central regions) in the trigeminal ganglia (gV), in the newly formed statoacoustic ganglion (sag), in the gP, and the precursor of the medial lateral line and vagal ganglia (gM/X) (Fig. 1D; Liu et al., 2006a). Similar *cdh6* expression pattern was seen in the gV, sag, gM/X and gP of older embryos, and the later formed anterodorsal and anteroventral lateral line ganglia (gAd and gAv, respectively) also expressed *cdh6* (Fig. 1E and F; Liu et al., 2006a). After 21 hpf, no *cdh6* expression was detected in the migrating pPLL and neuromasts.

Blocking Cdh6 function affects formation of a subset of cranial ganglia

The specificity of the 2 translation blocking zebrafish *cdh6* MOs was previously characterized, showing reduced cadherin-6 protein (Cdh6) expression and *cdh6* mRNA rescue of morphant phenotype (Kubota et al., 2007; Liu et al., 2008a). Injection of either of *cdh6*MO1 or *cdh6*MO2 produced embryos with similar body and yolk size as uninjected control embryos (Fig. 2), with the morphants having gross morphological defects such as smaller eye, edema in the thorax, short yolk extension, and/or curved body (Fig. 2D and G; more obvious in embryos younger than 48 hpf, Fig. 2C, possibly due to disrupted kidney function, Kubota et al., 2007). In contrast, injection of the control MO (5-mismatched) resulted in embryos that were indistinguishable from uninjected control embryos. Effects of these *cdh6*MOs on the embryonic gross morphological defects were summarized in Table 1, which were similar to results from our previous study (Liu et al., 2008a). Embryos with severe gross morphological defects had much reduced head and eyes, curved and obviously smaller body, large thoracic edema, and large yolk. Embryos with moderate defects showed smaller eyes, moderate thoracic edema, straight or slightly curved body, with similar or slightly larger yolk compared to uninjected control embryos (Fig. 2). Mildly affected embryos looked similar to uninjected control embryos, except having obvious shortened yolk extensions. Most of these embryos also had slightly smaller eyes and enlarged thoracic edema upon careful examination. To make analysis and interpretation of results more consistent, differentiation of the cranial ganglia and lateral line system was examined in moderately affected embryos injected with *cdh6*MO2 (Liu et al., 2008a).

To further confirm the *cdh6*MO2 specificity, we performed *cdh6* mRNA rescuing experiments. Co-injection of the synthetic *cdh6* mRNA (150 pg/embryo) with *cdh6*MO2 (3.4 ng/embryo) resulted in most embryos (48–50 hpf) with either mild gross morphological defects or wild type appearance (30.0%; Table 1). Increasing *cdh6* mRNA dosage (300 pg + 3.4 ng *cdh6*MO2/embryo) increased the percentage of rescued embryos (55.1% wild type appearance; Fig. 2H, Table 1). Note that embryos injected with *cdh6* mRNA alone (300 ng/embryo; Fig. 2F) were indistinguishable from uninjected control embryos (Fig. 2E, Table 1).

Differentiation of the cranial and lateral line ganglia was analyzed using anti-HuC/D at 32 and 50 hpf. This antibody strongly labels cell bodies in the trigeminal ganglion (gV), anterodorsal lateral line ganglion (gAd), statoacoustic ganglion (sag) and posterior lateral line ganglion from 24 to 72 hpf zebrafish embryos (Raible and Kruse, 2000). It also labels the anteroventral lateral line ganglion (gAv, 36 hpf to 72 hpf) and vagal ganglion (gX, 45 hpf to 72 hpf). The staining intensity of the ganglia was similar between the control embryos and *cdh6* morphants, but organization, size and/or shape of several ganglia were different between these embryos (Fig. 3). At 32 hpf, the gV of control embryos was a compact and triangularly shaped structure (Fig. 3A; Raible and Kruse, 2000), whereas in most morphants the gV was irregularly shaped and fragmented (Fig. 3F, Table 2), although there was no significant difference in their size (Fig. 3K). The gAd in control embryos was oval shaped (Fig. 3A, Raible and Kruse, 2000), while most of the *cdh6* morphant gAd was elongated, and slightly smaller than control embryos (Fig. 3F). The staining intensity was different between the anterior half (stronger) and posterior half (weaker) of the sag in both the control (Fig. 3A) and morphant embryos (Fig. 3F), and the ganglion had similar shape (a large anterior that tapers off in the posterior) in these embryos. But the morphant sag was significantly smaller than the control sag. There was no consistent difference in the size and shape of the gP between the control embryos and morphants (Fig. 3A & F): there was no significant difference in gP size at 32 hpf, while the morphant gP was slightly (statistically significant) larger than control gP at 50 hpf. Similar results for the sag and gAd were obtained using *NeuroD* and zn5 immunostaining. At 32 hpf, a *NeuroD* expressing area is located anteromedial to the otic vesicle, which includes the gAv, facial ganglion and sag (Andermann et al., 2002). This area in control embryos was significantly larger than that in *cdh6* morphants, although it had similar shape and staining intensity (Fig. 4). Compared to the gAd in control embryos (Fig. 4A), the morphant gAd was more elongated and its staining was weaker. The gP and precursors of the gX are also *NeuroD* positive (Andermann et al., 2002) (gX precursors are not labeled with anti-HuC/D staining), and they were also smaller and stained weaker in the morphants (Fig. 4). Zn5 labels both soma and processes of a subset of neurons in the gV, gAd and sag (Liu et al., 2008b). Similar to the above results, zn5 labeled morphant sag appeared smaller than control sag (Fig. 5). But unlike the results from the anti-HuC/D staining, the zn5 labeled gV area was smaller in most morphants at 32 hpf (Fig. 5A & E, Table 2). The difference may at least partially due to disrupted gV differentiation (e.g. affected neuronal processes formation) in the morphants, and/or difference in proteins recognized by these two antibodies.

By 50 hpf, the gV and gAd partially fuse (Higashijima et al., 2000; Raible and Kruse, 2000). Like the younger *cdh6* morphants, the gV was disorganized and fragmented (Fig. 3D)

compared to that of control embryos (Fig. 3B) or embryos injected with the 5-mismatched MO (Fig. 3C). Again, no significant difference in gV/Ad size was detected (Fig. 3L). Like the younger *cdh6* morphants, the sag (Fig. 3I), although similar in shape and staining to that of control embryos (Fig. 3G), was significantly smaller than control sag (Fig. 3L). To ensure that ganglia area measurements are consistent with changes in three-dimensional ganglia volumes, we measured sag volume in 50 hpf embryos using laser scanning confocal microscopy and Volocity image analysis software (Perkin Elmer). Whole mount anti-HuC/D immunofluorescence staining was used to measure average sag volume. Control sag volume (46,412 cubic microns, SD=5,220, n=5) was significantly larger than that in *cdh6* morphant embryos (29,425 cubic microns, SD=4,252, n=7; P>0.0001), similar to the area measurements. At 50 hpf, the gX has become a distinct large ganglion situated ventral to the gP (Fig. 3B), but the morphant gX (Fig. 3D) was only about half the size as that of the control embryos (Fig. 3L). Similar to the younger embryos, the gP at 50 hpf showed similar staining in control (Fig. 3B) and morphant embryos (Fig. 3D), and the gP was slightly larger in the morphant embryos (Fig. 3L). These results were complimentary with results obtained using zn5 immunostaining (Fig. 5). At 50 hpf, the zn5 stained sag were triangularly shaped in both control (Fig. 5F) and morphant embryos (Fig. 5G), but the morphant sag was obviously smaller. The labeling of the morphant gX (Fig. 5C) was apparently weaker compared to that of control embryos (Fig. 5B).

To test whether morphant embryos were delayed in overall development, we measured the otic vesicle size, which becomes larger as development proceeds (Haddon and Lewis, 1996), and we found that the morphant embryo inner ear size was similar in to that of control embryos (Fig. 3L).

Cranial and lateral line ganglia defects in cdh6 morphants were rescued by cdh6 mRNA injection

Co-injection of the synthetic *cdh6* mRNA with *cdh6*MO2 resulted in most embryos with wildtype gross morphology or with gross morphological defects that were less severe than embryos injected with only *cdh6*MO2 (see above, Table 2). To determine whether or not rescue of gross morphology was accompanied with cranial and lateral line ganglia phenotype rescue, we compared control, morphant and rescue embryos using anti-HuC/D and zn5 antibody staining (Figs. 3 & 5). Embryos with wild type gross morphology also had anti-HuC/D (Fig. 3E & J) zn5 (Fig. 5D & H) staining patterns that were indistinguishable from those of control embryos (Figs. 3B & G, 5B & F; Table 2). Moreover, measurements of anti-HuC/D-labeled cranial and lateral line ganglia of the rescued embryos showed that they were similar in size to the control values in all the labeled ganglia (Fig. 3L). Therefore, ganglia development was rescued, like gross morphological features in embryos co-injected with *cdh6*MO2 and *cdh6* mRNA. These data indicate that the *cdh6* morphant phenotype is specific, that is, cranial ganglia defects are due to *cdh6* loss-of-function.

Analysis of apoptosis cdh6 morphants

To determine whether the smaller sag and vagal ganglion in *cdh6* morphants was mainly due to increased cell death, we performed TUNEL staining (Fig. 6). At 24 hpf, control and *cdh6* morphant embryos showed no statistical difference in TUNEL-positive nuclei (n=10 each in

control and morphant groups; Fig. 6A,D). Of 10 *cdh6* morphants examined at 35 hpf, only three apoptotic cells (all in one embryo) were detected in the otic vesicle and surrounding hindbrain area (Fig. 6E). Similar results were observed in older (50 hpf) *cdh6* morphants (10 embryos examined in the otic vesicle and surrounding area, 2 apoptotic cells, both in one embryo; Fig. 6F). These results were similar to uninjected control embryos (Fig. 6B and D; 10 embryos examined for each stage). For both control and morphant embryos, there were numerous apoptotic cells in the fore- and midbrain (Fig. 6G and I) and trunk and tail regions of these embryos (Fig. 6H and J).

cdh6 function in cranial and lateral line nerves development

Defects in *cdh6* morphant cranial and lateral line ganglia suggest that development of their nerves may also be affected. Formation of these nerves was analyzed using anti-acetylated tubulin immunostaining (Raible and Kruse, 2000). At 50 hpf, in both control embryos and embryos injected with the 5-mismatched MO, several distinct nerves were observed originating from the gV/Ad, projecting anterodorsally (e.g. the anterodorsal lateral line nerve (nADso) and the dorsolateral nerve of the trigeminal ganglion (nVDl, Fig. 7A & B; Raible and Kruse, 2000), or anteroventrally (e.g. the buccal ramus of the anterodorsal lateral line nerve (nADb) and the mandibular ramus of the anteroventral lateral line nerve (nAVm, Fig. 7A & B). These nerves were also present in most *cdh6* morphants (Fig. 7C), and the nADb appeared to be similar as in the control embryos. However, the other nerves were different: the nADso and nVDl were more convoluted and displayed varicosities, a beaded appearance, while the nAVm was shorter and less fasciculated. The vagal nerve (nX) in control embryos or embryos injected with the 5-mismatched MO was conspicuous with a central projecting vagal root (rX) and four peripheral branches (Fig. 5A & B; Table 3; Raible and Kruse, 2000). In the *cdh6* morphants, the rX was thinner, and the nX contained only two branches (the most anterior and posterior branches), and the nX stem (before the nerve branches) was defasciculated (Fig. 5C). The posterior lateral line nerve (which originates from the gP and is located lateral to the horizontal myoseptum) is a straight nerve extending from the gP to the tail in control embryos at 50 hpf (Fig. 8). The morphant nP had similar appearance as that in the control embryos, except that it appeared to be a little thinner in most of the morphants (14/18), but it reached the tail region in most (15/18) morphants examined (Fig. 8; Table 3). Confocal microscopy was performed to ensure that changes observed in wide field microscopy were not merely due to lack of sensitivity, and these experiments confirmed the *cdh6* loss-of-function phenotypes, particularly the gV/Ad disorganization and nX branching (Fig. 7D–G).

Discussion

There is extensive information on cadherins function in development of the vertebrate central nervous system. Cadherins are involved in numerous events during the vertebrate brain development, including formation and maintenance of the neuroepithelium, differentiation and migration of neurons, neurite initiation, outgrowth, pathfinding, fasciculation, synapse formation and stabilization (Hirano et al., 2003; Suzuki and Takeichi, 2008). Only a few studies focused on cadherins roles in the development of the vertebrate cranial ganglia or lateral line system. We previously showed that cadherin-2 (Cdh2) and

cadherin-4 (Cdh4) play distinct roles in differentiation of these structures (Kerstetter et al., 2004; Wilson et al., 2007). More recently, Lamora and Voigt (2009) discovered that Cdh2 functions cell autonomously in guiding afferent fibers to their targets in zebrafish cranial sensory ganglia (e.g. facial ganglion and gX), and Shiau and Bronner-Fraser (2009) demonstrated that Cdh2 works in concert with Slit1-Robo2 signaling in regulating formation of placode-derived cranial sensory ganglia (e.g. gV).

The *cdh6* loss-of-function phenotype in this study correlates well with *cdh6* expression data (Fig. 1; Liu et al., 2006a). Reducing Cdh6 function using the morpholino technique produced distinct defects in most cranial and lateral line ganglia that express *cdh6*. The ganglia with strong *cdh6* expression (e.g. sag and gX) exhibited significant reduction in size. There was no detectable difference in the gV size between the control and morphant embryos, with this ganglia expressing *cdh6* only in a subset of cells located in peripheral regions. It is possible that these *cdh6* expression cells in the gV participate in assembly of this ganglion, because the morphant gV was disorganized and fragmented. It is interesting that no obvious defect is found in the morphant gP and only a small defect in the nP (thinner), although the gP contains high levels of *cdh6* throughout embryonic development. This may be due to compensatory function of other cadherins expressed in the gP, including, *cdh2*, *cdh4* and *cdh10* (Liu et al., 2001; 2003; 2006a).

Cdh6 is likely to function in a direct and specific mechanism during cranial ganglia and nerve formation. Supporting this idea, *cdh6* expression in the central nervous system of 1–2 day old zebrafish embryos is restricted to patches in the dorsal and ventral forebrain, and dorsal hindbrain (Liu et al., 2006a). Importantly, *cdh6* expression in the hindbrain is confined to superficial regions of the cerebellum and medulla (Fig. 1A–E; Liu et al., 2006a), and application of zebrafish *cdh6* mRNA to *cdh6* MO injected embryos resulted in partial to complete rescue of the cranial and lateral line ganglia defects. Moreover, our data supports the idea that cranial and lateral line ganglia defects in *cdh6* morphant embryos are not due to a general delay in embryonic development: (i) morphant embryos had similar body and yolk sizes as control embryos; (ii) morphant embryos had similar otic vesicle size as control embryos; (iii) in morphant embryos, the nP reached the tail region around 48 hpf, like that of wild type zebrafish embryos (Metcalfe, 1985).

The *cdh6* loss-of-function phenotype is distinct from the *cdh2* loss-of-function phenotype (*cdh2* mutant *glo* or morphants, Kerstetter et al., 2004) or the *cdh4* phenotype (*cdh4* morphants, Wilson et al., 2007). *cdh2* is widely expressed in both the central and peripheral nervous structures in embryonic zebrafish (Bitzur et al., 1994; Liu et al., 2003). Functional analysis showed that *cdh2* participates in cranial ganglia and lateral line system development, but the *cdh2* morphants and *glo* mutant phenotypes are more severe including: (i) more severe fragmentation of the gV/Ad; (ii) little or no dorsal nerve branches from the gV/Ad; (iii) altered shape, and greatly reduced sag; and (iiii) the gX nerves and nerve root were barely visible (Kerstetter et al., 2004). Although the posterior lateral line nerve (nP) was present in cdh2 morphants or *glo* mutants, the nerve had greatly altered trajectories (curved or turned around).

cdh4 was also detected in both the central and peripheral nervous structures of the embryonic zebrafish (Liu et al., 2001; 2003). *cdh4* expression in the cranial and lateral line ganglia is more restricted (e.g. after 30 hpf). It is not surprising that no obvious defects in these ganglia are found in 30 hpf *cdh4* morphant embryos (Wilson et al., 2007). At 50 hpf, several defects become evident in the ganglia and their nerves. The gV/Ad dorsal nerve branches are present, but thinner than control embryos (but lacking the varicosities seen in *cdh6* morphant gV/Ad dorsal nerve branches). The nADb, one of the ventral branches was also much thinner in *cdh4* morphants than control embryos (no obvious defects in this nerve in *cdh6* morphants). The reduced sag size and altered shape in *cdh4* morphant embryos are more severe than those of *cdh6* morphant embryos which are mainly reduced in size. Moreover, *cdh4* morphants have severely reduced nP length (reaches only ½ to 2/3 of the body length). In constrast, *cdh6* loss-of-function had little effect on nP length.

Despite the strong *cdh6* expression in most of the cranial and lateral line ganglia during critical stages of their development, defects in these structures of *cdh6* morphants are generally less severe than those of embryos with *cdh2* or *cdh4* loss-of-function (see above). This may partially be explained by compensatory function of other cadherins in these ganglia, such as *cdh2*, *cdh4* and *cdh10* (Liu et al., 2003; 2006b). Moreover, both *cdh2* and *cdh4* are widely expressed in the hindbrain of embryonic zebrafish. Therefore, defects in the cranial and lateral line ganglia and nerves in embryos lacking these cadherins' functions may display secondary defects due to hindbrain malformation (Lele et al., 2002; Hong and Brewster, 2006), which subsequently affects the cranial and lateral line ganglia differentiation. Because there is no increase in the number of apoptotic cells in the cranial and lateral line ganglia of 24, 32 and 50 hpf *cdh6* morphants, the reduced sizes in the sag and gX of *cdh6* morphants may due to decreased cell proliferation, similar to previous findings in the retina of zebrafish *cdh6* morphants (Liu et al., 2008a) and *Xenopus cdh6* loss-of-function embryos (Ruan et al., 2006). It is unclear how Cdh6 controls differentiation of the zebrafish cranial and lateral line structures. Like other classic cadherins, Cdh6 may mediate homotypic adhesion (via recognition and binding its N-terminus) that is necessary for cranial ganglia aggregation and differentiation, and cadherin adhesion may regulate extension and fasciculation of cranial nerves. Cdh6 may also regulate development and differentiation by regulating intracellular signaling mechanisms via cytoplasmic domain interacting with proteins like β–catenin, tyrosine kinases, and Rho-family GTPases (Wheelock and Johnson, 2003; Bruses, 2006). Understanding molecular mechanisms underlying *cdh6* function in the development of the cranial ganglia and lateral line system will be the focus future study.

Acknowledgments

We thank Dr. Tohru Murakami (Gunma University) for providing the zebrafish *cdh6* cDNA for the synthesis *cdh6* mRNA, and Deborah Stenkamp (University of Idaho) for providing the *NeuroD* cDNA. This study was supported by grants from the NIH to J.A.M. (RO1 DC006436) and Q.L. (R15 EY13879).

References

Andermann P, Ungos J, Raible DW. Neurogenin1 defines zebrafish cranial sensory ganglia precursors. Dev Biol. 2002; 251:45–58. [PubMed: 12413897]

Babb-Clendenon SG, Shen Y, Liu Q, Turner KE, Mills MS, Barald KF, Marrs JA. Cadherin-2 controls morphogenesis of the zebrafish inner ear. J Cell Sci. 2006; 119:5169–5177. [PubMed: 17158919]

Bruses JL. N-cadherin signaling in synapse formation and neuronal physiology. Mol Neurobiol. 2006; 33:237–252. [PubMed: 16954598]

Cho EA, Patterson LT, Brookhiser WT, Mah S, Kintner C, Dreesler GR. Differential expression and function of cadherin-6 during renal epithelium development. Development. 1998; 125:803–812. [PubMed: 9449663]

David R, Wedlich D. *Xenopus* cadherin-6 is expressed in the central andperipheral nervous system and in neurogenic placodes. Mech Dev. 2000; 97:187–190. [PubMed: 11025223]

Gumbiner BM. Regulation of cadherin-mediated adhesion in morphogenesis. Nature Rev. 2005; 6:622–634.

Haddon C, Lewis J. Early ear development in the embryo of the zebrafish, *Danio rerio*. J Comp Neurol. 1996; 365:113–128. [PubMed: 8821445]

Hall, BK. The neural crest in development and evolution. New York: Springer-Verlag; 1999.

Hirano S, Suzuki ST, Redies C. The cadherin superfamily in neural development: diversity, function and interaction with molecules. Front Biosci. 2003; 8:d306–d355. [PubMed: 12456358]

Hong E, Brewster R. N-cadherin is required for the polarized cell behaviours that drive neurulation in the zebrafish. Development. 2006; 133:3895–3905. [PubMed: 16943271]

Kelsh RN, Raible DW. Specification of zebrafish neural crest. Results Probl Cell Differ. 2002; 40:216–236. [PubMed: 12353478]

Kerstetter AE, Azodi E, Marrs JA, Liu Q. Cadherin-2 function in the cranial ganglia and lateral line system of developing zebrafish. Dev Dyn. 2004; 230:137–143. [PubMed: 15108318]

Kim WY, Fritzsch B, Serls A, Bakel LA, Huang EJ, Reichardt LF, Barth DS, Lee JE. NeuroD-null mice are deaf due to a severe loss of the inner ear sensory neurons during development. Development. 2001; 128:417–426. [PubMed: 11152640]

Kimmel CB, Ballard WW, Kimmel SR, Ullmann B, Schilling TF. Stages of embryonic development of the zebrafish. Dev Dyn. 1995; 203:253–310. [PubMed: 8589427]

Knaut H, Blader P, Strahle U, Schier AF. Assembly of trigeminal sensory ganglia by chemokine signaling. Neuron. 2005; 47:653–666. [PubMed: 16129396]

Kubota F, Murakami T, Mogi K, Yorifuji H. Cadherin-6 is required for zebrafish nephrogenesis during early development. Int J Dev Biol. 2007; 51:123–129. [PubMed: 17294363]

Lamora A, Voigt MM. Cranial sensory ganglia neurons require intrinsic N cadherin function for guidance of afferent fibers to their final targets. Neurosci. 2009; 159:1175–1184.

Lele Z, Folchert A, Concha M, Rauch G-J, Geisler R, Rosa F, Wilson SW, Hammerschmidt M, Bally-Cuif L. parachute/n-cadherin is required formorphogenesis and maintained integrity of the zebrafish neural tube. Development. 2002; 129:3281–3294. [PubMed: 12091300]

Liu Q, Marrs JA, Chuan JC, Raymond PA. Cadherin-4 expression in the zebrafish central nervous system and regulation by ventral midline signaling. Dev Brain Res. 2001; 131:17–29. [PubMed: 11718832]

Liu Q, Ensign RD, Azodi E. Cadherin-1, 2 and –4 expression in the cranial ganglia and lateral line system of developing zebrafish. Gene Expr Patt. 2003; 3:651–656.

Liu Q, Liu B, Wilson AL, Rostedt J. *cadherin-6* message expression in the nervous system of developing zebrafish. Dev Dyn. 2006a; 235:272–278. [PubMed: 16258934]

Liu Q, Duff RJ, Liu B, Wilson AL, Babb-Clendenon SG, Francl J, Marrs JA. Expression of *cadherin-10*, a type II classic cadherin gene, in the nervous system of the embryonic zebrafish. Gene Expr Patt. 2006b; 6:703–710.

Liu Q, Londraville RL, Marrs JA, Wilson AL, Mbimba T, Murakami T, Kubota F, Zheng W, Fatkins DG. Cadherin-6 function in zebrafish retinal development. Dev Neurobiol. 2008a; 68:1107–1122. [PubMed: 18506771]

Liu Q, Marrs JA, Londraville RL, Wilson AL. Cadherin-7 function in zebrafish development. Cell and Tissue Res. 2008b; 334:37–45. [PubMed: 18665394]

Lopez-Schier H, Starr CJ, Kappler JA, Kollmar R, Hudspeth AJ. Directional cell migration establishes the axes of planar polarity in the posterior lateral-line organ of the zebraish. Dev Cell. 2004; 7:401–412. [PubMed: 15363414]

Ma Q, Chen Z, del Barco Barrantes I, de la Pompa JL, Anderson DJ. Neurogenin1 is essential for the determination of neuronal precursors for proximal cranial sensory ganglia. Neuron. 1998; 20:469–482. [PubMed: 9539122]

Mah SP, Saueressig H, Goulding M, Kintner C, Dressler GR. Kidney development in cadherin-6 mutants: delayed mesenchyme-to-epithelial conversion and loss of nephrons. Dev Biol. 2000; 223:38–53. [PubMed: 10864459]

Metcalfe WK. Sensory neuron growth cones comigrate with posterior lateral line primordial cells in zebrafish. J Comp Neurol. 1985; 238:218–224. [PubMed: 4044912]

Nollet F, Kools P, van Roy F. Phylogenetic analysis of the cadherin superfamily allows identification of six major subfamilies besides several solitary members. J Mol Biol. 2000; 299:551–572. [PubMed: 10835267]

Northcutt RG, Gans C. The genesis of neural crest and epidermal placodes: A reinterpretation of vertebrate origins. Q Rev ZBiol. 1983; 58:1–28.

Paul R, Necknig U, Busch R, Ewing CM, Hartung R, Isaacs WB. Cadherin-6: a new prognostic marker for renal cell carcinoma. J Urol. 2004; 171:97–101. [PubMed: 14665853]

Raible DW, Kruse GJ. Organization of the lateral line system in embryonic zebrafish. J Comp Neurol. 2000; 421:189–198. [PubMed: 10813781]

Ruan G, Wedlich D, Koehler A. *Xenopus* cadherin-6 regulates growth and epithelial development of the retina. Mech Dev. 2006; 123:881–892. [PubMed: 17034995]

Shiau CE, Bronner-Fraser M. N-cadherin acts in concert with Slit1-Robo2 signaling in regulating aggregation of placode-derived cranial sensory neurons. Development. 2009; 137:4155–4164. [PubMed: 19934013]

Suzuki SC, Takeichi M. Cadherins in neuronal morphogenesis and function. Dev Growth Differ Suppl. 2008; 1:S119–S130.

Takeichi M. Cadherin cell adhesion receptors as a morphogenetic regulator. Science. 1991; 251:451–455.

Westerfield, M. The zebrafish Book. Eugene, OR: University of Oregon Press; 2005.

Wheelock MJ, Johnson KR. Cadherin-mediated cellular signaling. Cur Opin Cell Biol. 2003; 15:509–514.

Wilson A, Shen Y, Babb-Clendenon SG, Rostedt J, Liu B, Barald KF, J.A. Marrs JA, Liu Q. Cadherin4 plays a role in the development of zebrafish cranial ganglia and lateral line system. Dev Dyn. 2007; 236:893–902. [PubMed: 17279575]

Xiang YY, Tanaka M, Suzuki M, Igarashi H, Kiyokawa E, Naito Y, Ohtawara Y, Shen Q, Sugimura H, Kino I. Isolation of complementary DNA encoding K-cadherin, a novel rat cadherin preferentially expressed in fetal kidney and kidney carcinoma. Cancer Res. 1994; 54:3034–3041. [PubMed: 8187093]

Yagi T, Takeichi M. Cadherin superfamily genes: functions, genomic organization, and neurologic diversity. Genes & Development. 2000; 14:1169–1180. [PubMed: 10817752]

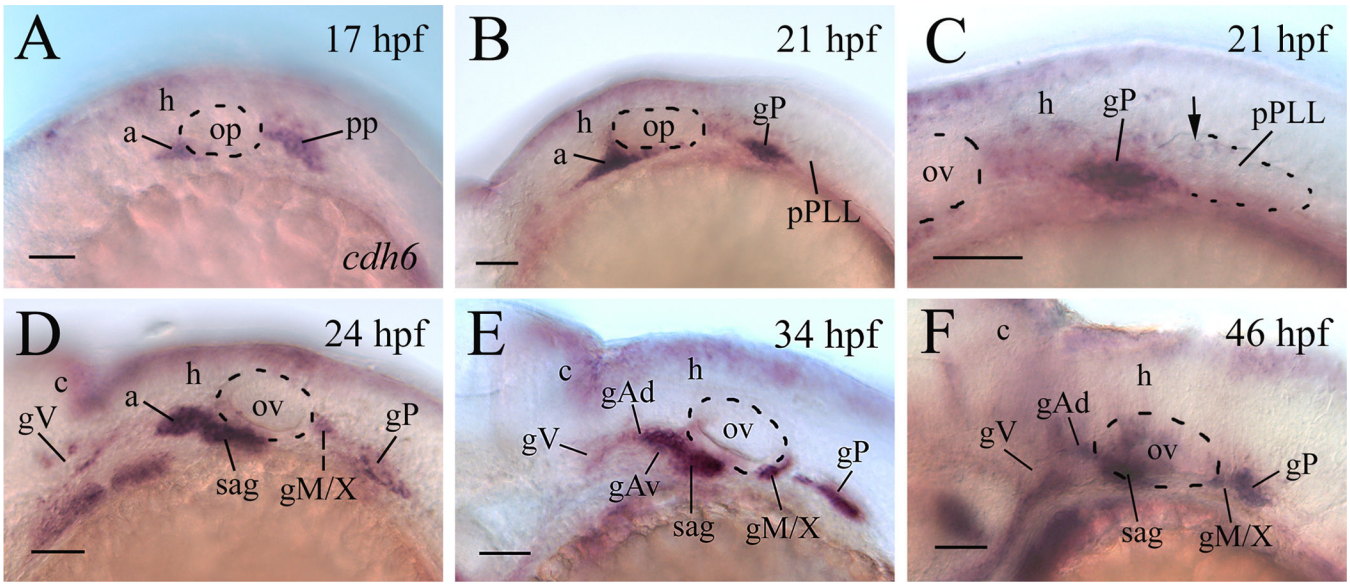

Figure 1.

cdh6 expression in the cranial and lateral line ganglia of embryonic zebrafish. All panels show lateral views of the hindbrain region of whole mount embryos (anterior to the left and dorsal up) processed for in situ hybridization using a *cdh6* cRNA probe. Panel C is a higher magnification of the post otic area showing the newly formed primordium of the post lateral line (pPLL, dashed line indicating the boundary of its posterior 2/3). The arrow points to one of a few *cdh6* expressing cells in the pPLL. Other abbreviations: a, anterior lateral line placode area; c, cerebellum; gAd, anterodoral lateral line ganglion; gAv, anteroventral lateral line ganglion; gM/X, medial lateral line and vagal ganglia; gP; posterior lateral line ganglion; gV, trigeminal ganglion; h, hindbrain; op, otic placode; ov, otic vesicle (indicated by the dashed line); PP, postotic placode; sag, statoacoustic ganglion. Scale bar = 50 μm.

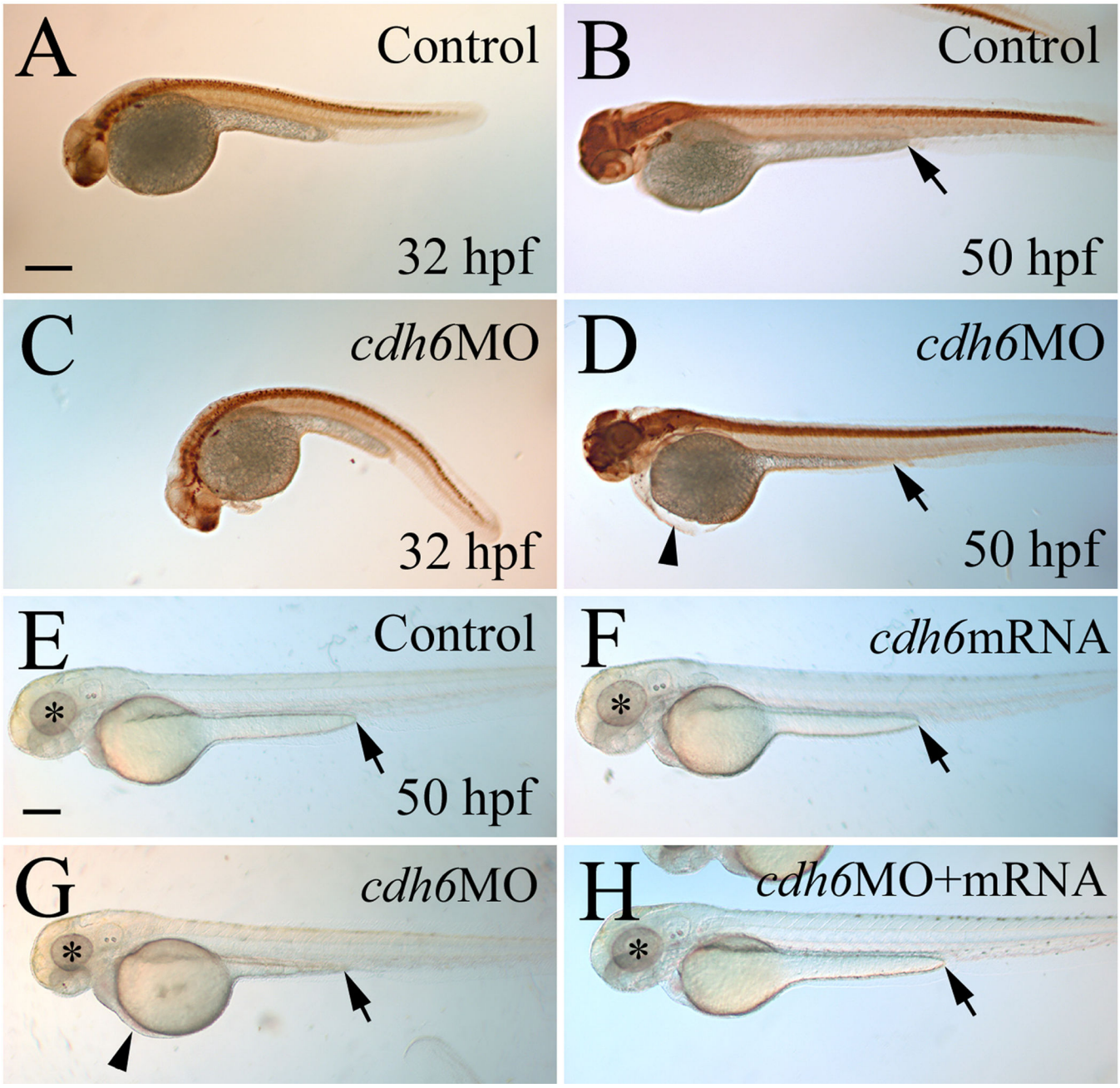

Figure 2.

Overall *cdh6* loss-of-function phenotype. Lateral views (anterior to the left and dorsal up) of whole mount embryos processed for anti-HuC/D immunoperoxidase staining. The morphants (panels C and D, injected with *cdh6*MO2 showing moderate phenotype) were similar in body and yolk size as uninjected control embryos (panels A and B), but had smaller head and eyes, curved body at younger (e.g. 32 hpf) stages, shortened yolk extension and edema in the thorax, as shown in our previous publication (Liu et al., 2008a). Panels E-H show live embryos raised in PTU treated fish water. The eyes are indicated by asterisks,

edema in the thorax is indicated by an arrowhead, and the end of the yolk extension is indicated by an arrow. Scale bar = 250 μm for all panels.

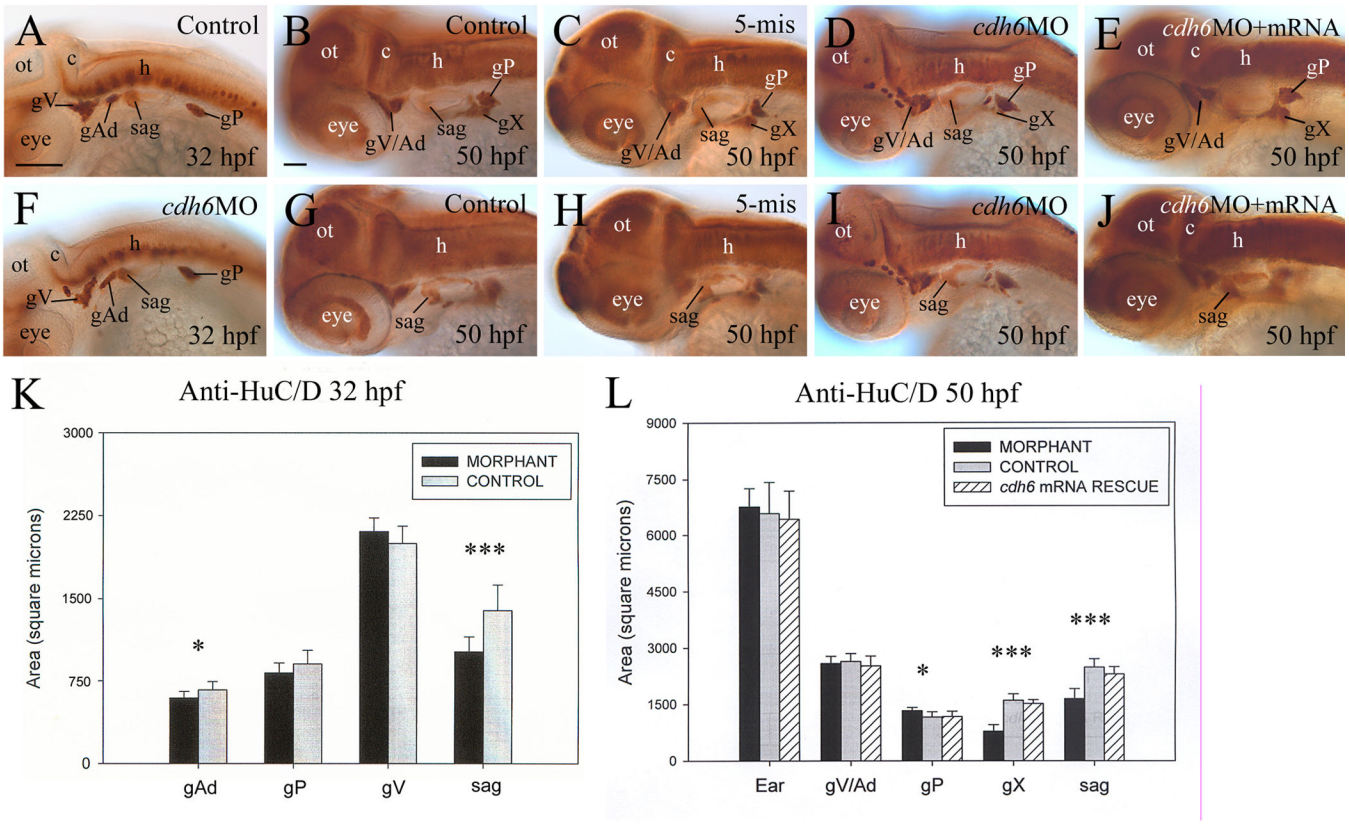

Figure 3.

Development of the cranial and lateral line ganglia requires Cdh6 function. Panels A–J show anti-HuC/D immunoperoxidase staining of embryos, showing lateral views (anterior to the left and dorsal up) of the head region. Panels K and L show histograms representing the area/size (square microns; n=13 for all measured ganglia) of anti-HuC/D labeled cranial and lateral line ganglia, comparing control embryos (gray bars), *cdh6* morphants (dark bars) and *cdh6* mRNA rescued embryos (bars with diagonal lines). One asterisk indicates significant difference ($p=0.0013$), while three asterisks indicate highly significant difference ($p<0.001$). Abbreviations: gX, vagal ganglion; ot, optic tectum. Other abbreviations are the same as in Figure 1. Panels A and F have the same magnification (scale bar = 100 μm), while the remaining panels have the same magnification (scale bar = 50 μm).

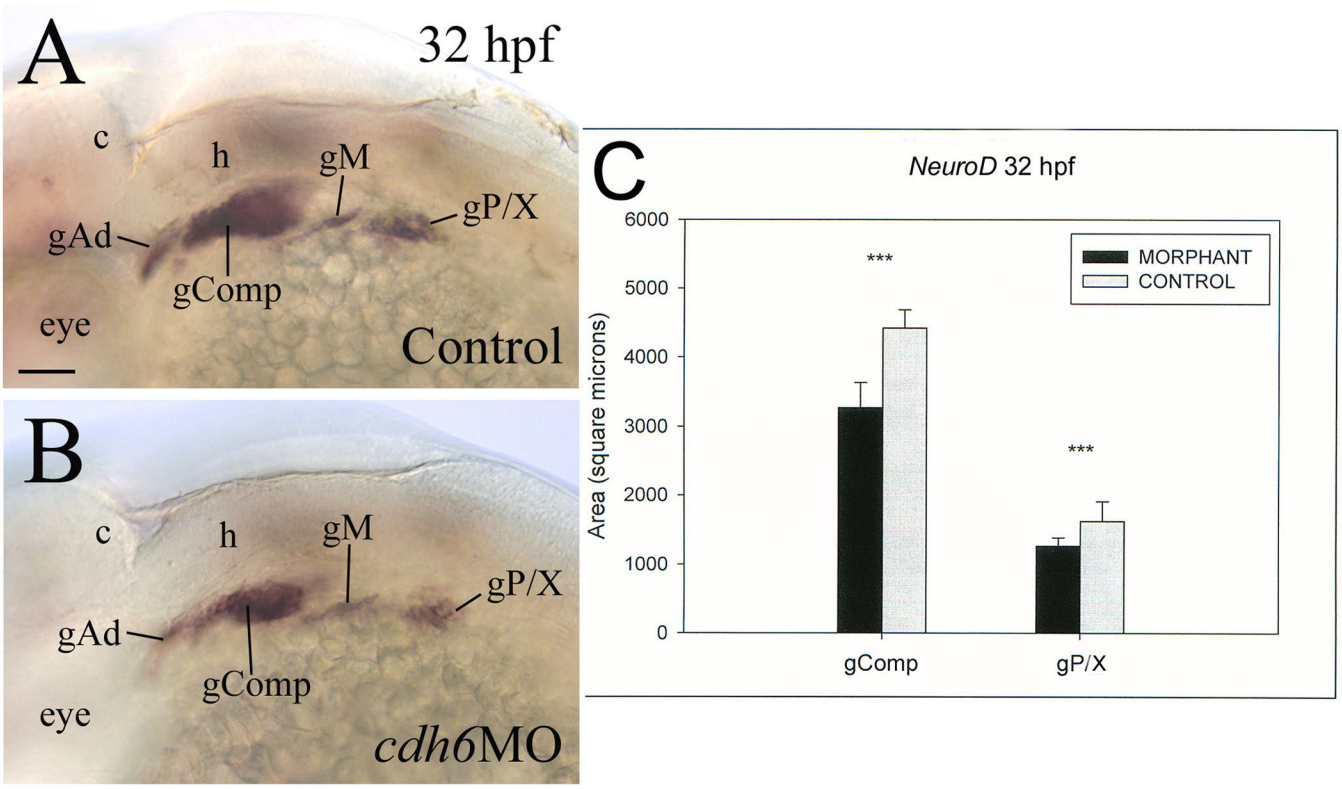

Figure 4.

Cdh6 function is required for differentiation of *NeuroD* positive cranial and lateral line ganglia. Panels A and B show lateral views (anterior to the left and dorsal up) of the hindbrain region of whole mount embryos processed for in situ hybridization using the neuroD cRNA probe. Panel C show comparisons in area size of two *neuroD* labeled areas between control (gray bars) and cdh6 morphants (dark bars). Abbreviations: gComp, complex “ganglion” including the facial ganglion, anteroventral lateral line ganglion and statoacoustic ganglion; gM, middle lateral line ganglion; gP/X, posterior lateral line ganglion and precursors of vagal ganglion. Other abbreviations are the same as Figure 1. Scale bar = 50 μm.

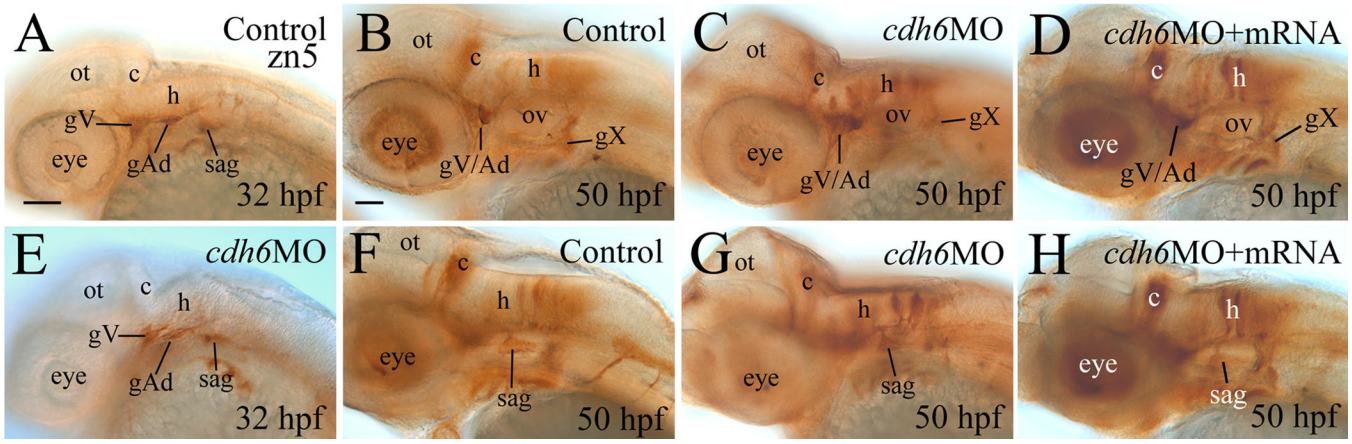

Figure 5.

Cdh6 function is required for differentiation of zn-5 positive cranial and lateral line ganglia. All panels are lateral views (anterior to the left and dorsal up) of the head region of whole mount embryos. Abbreviations are the same as in Figure 1. All images have the same magnification. Scale bar = 50 μm.

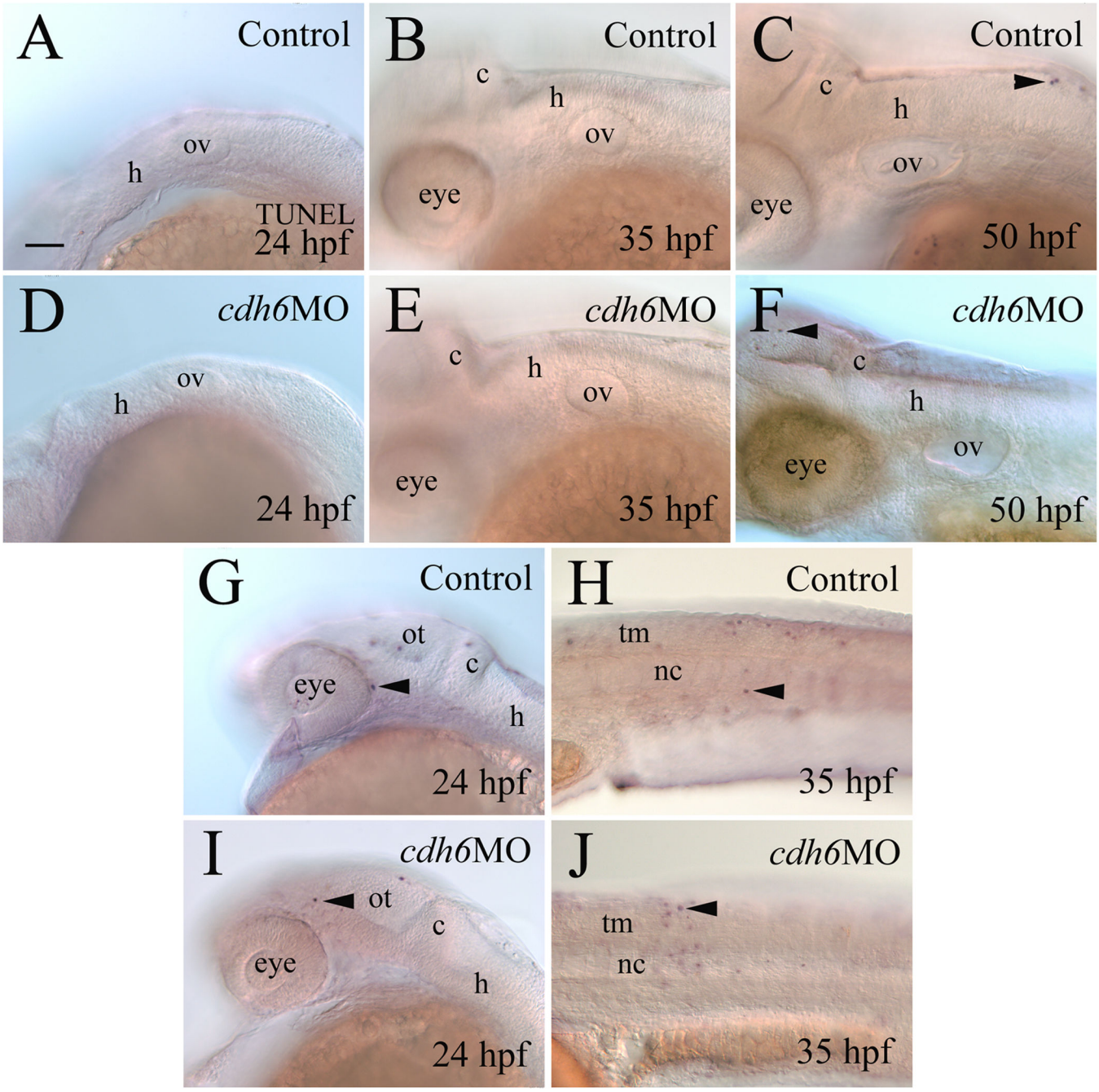

Figure 6.

Apoptosis analysis using TUNEL staining. All panels show lateral views of whole mount embryos (anterior to the left and dorsal up) processed for TUNEL staining. Panels A-F and G and I show the mid- and hindbrain region focusing on the otic vesicle, while panels H and J are from the body trunk region. Arrowheads point to some TUNEL positive cells. Abbreviation: nc, notochord; tm, trunk muscles. Other abbreviations are the same as in Figure 1. Scale bar = 50 μm for all panels.

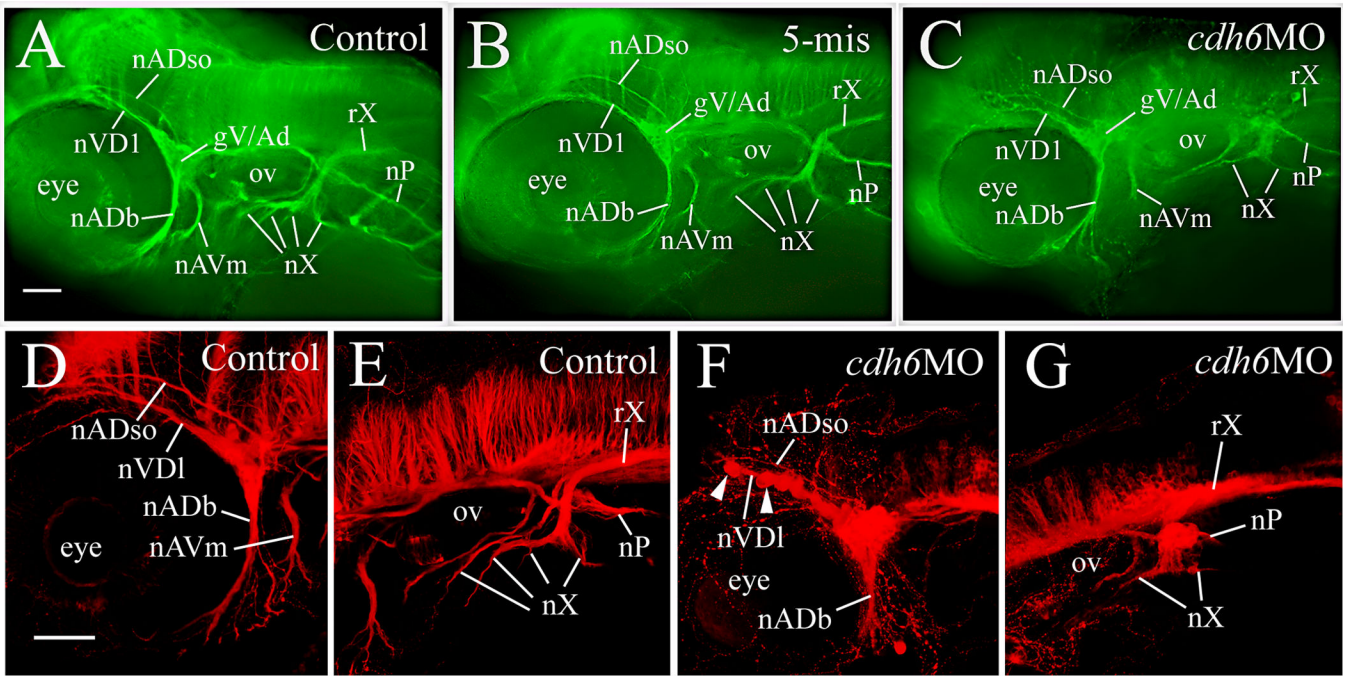

Figure 7.

cdh6 loss-of-function defects in cranial and lateral line nerves, demonstrated by anti-acetylated tubulin immunofluorescent staining, in a control embryo (panel A), an embryo injected with the 5-mismatched MO (panel B), and a cdh6 morphant (panel C). The images are lateral views (anterior to the left and dorsal up) of the head region of the whole mount embryos. Laser scanning confocal microscopy image projections confirmed results using wide field microscopy: anterior cranial nerves (panels D and F) and posterior cranial nerves (panels E and G) in control (panels D and E) and *cdh6* morphant (panels F and G) embryos. Arrowheads in panel F point to two of the cell clusters of the fragmented gV/Ad. The morphant vagus root (rX, panel G) was difficult to discern because it is situated above anti-acetylated tubulin positive brain cells and fiber tracks. Other abbreviations: nADb, buccal ramus of the anterodorsal lateral line nerve; nADso, superior ophthalmic ramus of the anterodorsal lateral line nerve; nAVm, mandibular ramus of the anteroventral lateral line nerve; nVDl, dorsolateral nerve of the trigeminal ganglion; nP, posterior lateral line nerve; nX, vagus nerves; ov, otic vesicle. All images have the same magnification.

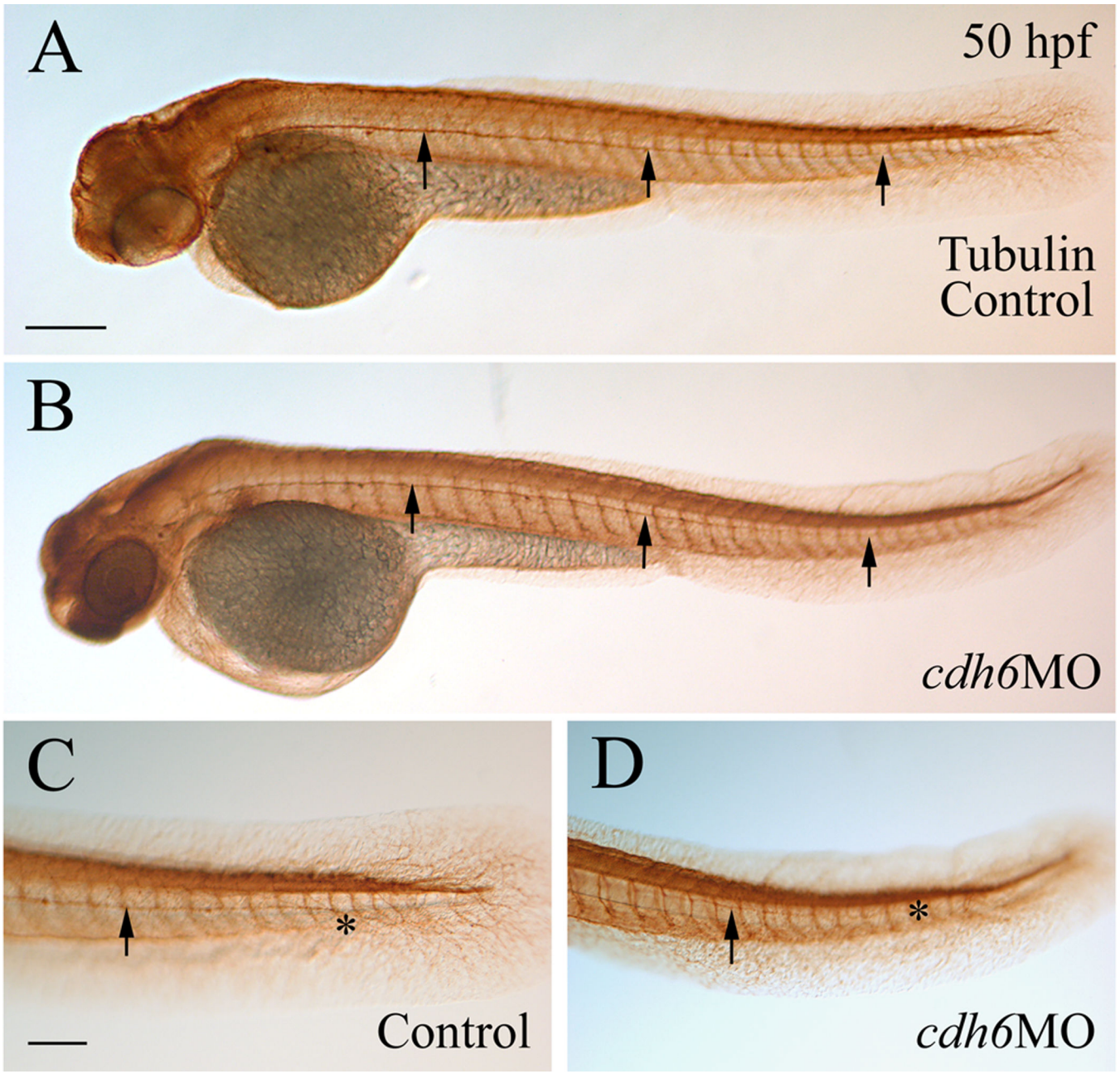

Figure 8.

Normal development of the posterior lateral line nerve in *cdh6* morphants. All panels show lateral views of whole mount embryos (anterior to the left and dorsal up) processed for anti-acetylated tubuline immunoperoxidase staining. Arrows point to the posterior lateral line nerve, while the asterisk indicates the terminus of the nerve. Panels C and D are higher magnifications (same magnification) of the tail region of the embryos in panels A and B (same magnification), respectively. Scale bar = 200 μm for panels A and B, 100 μm for panels C and D.

Table 1

Effects of *cdh6*MO Injection on Zebrafish Development

	# embryos with slight gross defects (%)	**# embryos with moderate gross defects (%)**	**# embryos with severe gross defects (%)**	**# embryos examined at 48–50 hpf (# embryos with no phenotype)**
Uninjected Control	10 (3.6%)	7 (2.5%)	9 (3.2%)	281 (255)
*cdh6*MO1 (6.0 ng)	27 (20.6%)	86 (65.6%)	12 (9.2%)	131 (6)
*cdh6*MO2 (3.4 ng)	57 (13.2%)	316 (73.1%)	37 (8.6%)	432 (22)
5-misMO (6.0 ng)	4 (2.7%)	5 (3.3%)*	2 (1.3%) *	149 (138)
*cdh6*MO2 (3.4 ng) and *cdh6* mRNA (150 pg)	32 (53.3%)	10 (16.7%)	0 (0%)	60 (18)
*cdh6*MO2 (3.4 ng) and *cdh6* mRNA (300 pg)	28 (35.9%)	5 (6.4%)	2* (2.6%)	78 (43)
cdh6 mRNA (300 pg)	4 (7.1%)	0 (0%)	0 (0%)	56 (52)

*The gross morphological defects in these embryos (e.g. little dorsal structures or truncated bodies) were different from the *cdh6*morphant

Table 2

Effects of *cdh6*MO Injection on Cranial and Lateral Line Ganglia Development

	gV/Ad (%)	sag (%)	gX (%)	gP (%)
32 hpf anti-Hu				
Control (n=30)	3.3	6.7		0
*cdh6*MO (n=30)	83.3	83.3		20
32 hpf zn5				
Control (n=30)	13.3	10		
*cdh6*MO (n=30)	83.3	80		
50 hpf anti-Hu				
Control (n=30)	10	6.7	16.7	3.3
5-misMO (n=24)	4.2	12.5	8.3	8.3
*cdh6*MO (n=30)	56.7	66.7	93.3	20
*cdh6*MO+mRNA (n=12)	0	16.7	8.3	0
50 hpf zn5				
Control (n=30)	0	13.3	6.7	
5-misMO (n=30)	10	16.7	10	
*cdh6*MO (n=28)	50	71.4	85.7	
*cdh6*MO+mRNA (n=1)	0	25.0	8.3	

n, number of ganglia examined. %, percentages of obviously abnormally formed ganglia (e.g. smaller size, altered shape, and/or reduced staining compared to the majority of control embryos).

Table 3

Effects of *cdh6*MO Injection on Cranial and Lateral Line Nerves Development

Anti-acetylated tubulin	gV/Ad nerves (%)	gX nerves (%)	nP (%)
Uninjected Control (n=18)	5.6	0	0
*cdh6*MO (n=18)	100	100	77.8*
5-misMO (n=16)	6.3	6.3	6.3

n, number of embryos examined.

* the morphant nP had similar appearance as control nP, and reached the tail region in most morphants, but most of the morphant nP (14/18) was thinner than control nP.